Heliyon 9 (2023) e13018

Contents lists available at ScienceDirect

Heliyon

journal homepage: www.cell.com/heliyon

Research article

NFATC1 and NFATC2 expression patterns in human osteochondromas

Yuanyuan Wang [a,b], Jiangdong Ren [c], Guojin Hou [d], Xianpeng Ge [a,b,*]

[a] Department of Stomatology, Xuanwu Hospital Capital Medical University, Beijing, China
[b] National Clinical Research Center for Geriatric Diseases, Beijing, China
[c] Department of Joint Surgery, Center for Orthopaedic Surgery, The Third Affiliated Hospital of Southern Medical University (Academy of Orthopaedics of Guangdong Province), Guangzhou, Guangdong, China
[d] Department of Orthopedics, Peking University Third Hospital, Beijing, China

ARTICLE INFO

Keywords:
Osteochondroma
Hereditary multiple exostoses
Periosteum
Periosteal progenitors
NFATC1
NFATC2

ABSTRACT

Background: Our previous study in genetic mouse models found that NFATc1 and NFATc2 suppress osteochondroma formation from entheseal progenitors. However, it remains unclear whether NFAT signaling is also involved in human osteochondromagenesis. As the first step in addressing this question, the current study aimed to determine the expression patterns of NFATC1 and NFATC2 in human osteochondroma samples.

Methods: Immunohistochemistry (IHC) was used to examine and analyze NFATC1 and NFATC2 expression in human osteochondroma samples. The human periosteum was used to map the expression of NFATC1 under physiological conditions by IHC. Furthermore, human periosteal progenitors were isolated and identified from the periosteal tissues of bone fracture healing patients. The expression of NFATC1 in human periosteal progenitors was characterized by Western blotting compared to human bone marrow stromal cells (BMSC).

Results: The IHC results showed that the expression of NFATC1 was undetectable in most human osteochondromas cells, and only a small proportion of osteochondroma cells, especially clonally grown chondrocytes, showed positive staining of NFATC1. NFATC2 expression was also undetectable in most chondrocytes in human osteochondromas. The mouse and human periosteum showed a comparable ratio of NFATC1 positive cells (9.56 ± 0.80% *vs* 11.04 ± 2.05%, $P = 0.3101$). Furthermore, Western blotting analysis revealed that NFATC1 expression was highly enriched in human periosteal progenitors compared to BMSC.

Conclusions: NFATC1 and NFATC2 are undetectable in most human osteochondroma chondrocytes. The expression pattern of NFATC1 in human osteochondromas and the normal periosteum suggests that NFAT signaling could be suppressed during human osteochondromagenesis.

1. Introduction

The nuclear factor of activated T cell (NFAT) transcription factor family includes five members (NFATc1-NFATc4 and NFAT5) with a common DNA binding domain of approximately 300 amino acid residues [1,2]. NFAT signaling was initially identified in T cells more than 30 years ago and played a critical role in regulating T cell differentiation and functions [3,4]. In addition to the immune system,

* Corresponding author. Department of Stomatology, Xuanwu Hospital Capital Medical University, Beijing, China.
E-mail addresses: xianpeng.ge@xwhosp.org, xpge@penggegroup.com (X. Ge).

https://doi.org/10.1016/j.heliyon.2023.e13018
Received 11 October 2022; Received in revised form 5 January 2023; Accepted 12 January 2023
Available online 18 January 2023

NFAT members are expressed in many other tissues and organs and play broad biological functions in various physiological and pathological processes, including cardiac valve development, skeletal muscle fiber differentiation, degenerative neural diseases, and osteoarthritis [3,5]. In the skeletal system, NFAT signaling has been widely characterized for its roles in osteoclast and osteoblast differentiation and functions [6–8].

Accumulating lines of evidence indicate that NFAT signaling also plays an important role in cartilage biology. As early documentation shows, NFATc2 null mice develop spontaneous extra-articular ectopic cartilaginous growth that undergoes endochondral ossification with age [9]. *Ex vivo* studies in the murine teratocarcinoma cell line ATDC5, primary epiphyseal chondrocytes and embryonic stem cells showed that NFAT signaling, particularly NFATc1, inhibits chondrogenesis [10–12]. Consistently, we recently found that *in vivo* ablation of NFATc1 in mouse entheseal progenitor cells leads to spontaneous osteochondroma formation at the enthesis of ligaments [13]. Meanwhile, NFATc1 and NFATc2 demonstrate complementary roles in determining the severity and number of mouse osteochondromas. Interestingly, cell lineage tracing data showed that NFATc1-expressing progenitors contribute to the formation of mouse enthesis and periosteum [13]. These findings uncover a previously unappreciated function of NFAT signaling as a suppressor of osteochondroma formation in entheseal/periosteal progenitors.

Osteochondromas are one of the most common bone tumors in humans, which can occur in both the appendicular and craniofacial bones [14–17]. These osteochondral tumors begin with ectopic cartilaginous outgrowths from entheseal/perichondrial progenitors on the bone surface. Mature osteochondromas are characterized by a cartilaginous cap with a marrow cavity continuous with that of the underlying bone [18–20]. Most osteochondromas occur solitarily, but these tumors can also occur in hereditary forms called multiple osteochondromas or hereditary multiple exostoses (HME). Osteochondromas, especially HME, can cause skeletal deformation, nerve and vesicular impingement, and psychological problems in children and adolescents. The most severe complication of osteochondromas is malignant transformation to secondary peripheral chondrosarcoma, which occurs in approximately 1% of solitary osteochondromas and 1–3% of patients with HME [21]. The pathogenesis of osteochondromas has been linked to loss-of-function mutations of the *EXT1* or/and *EXT2* genes, which encode Golgi-resident glycosyltransferases essential for the synthesis and assembly of extracellular heparan sulfate. In particular, the molecular mechanism of EXT genes that mediates osteochondroma formation remains poorly understood and not all osteochondromas can be detected with the mutation of EXT genes [22,23]. Our recent findings in NFATc1 and NFATc2 knockout mice indicate that impairment of NFAT signaling can also represent a cause of osteochondromagenesis [13]. However, whether NFAT signaling is also involved in human osteochondroma formation remains understudied.

In this study, as the first step in characterizing the role of NFAT signaling in human osteochondromagenesis, we examined the expression of NFATC1 and NFATC2 proteins in human osteochondroma samples. Our results showed an overall lack of expression of NFATC1 in most human osteochondroma cells, in contrast to enriched expression of NFATC1 in human periosteal progenitors. NFATC2 expression is also undetectable in most human osteochondroma chondrocytes. These results provide translational insights into previous findings on the role of NFATs in osteochondromagenesis and lay the groundwork for further studies on the mechanism of NFAT signaling that regulates human osteochondromagenesis.

2. Methods

2.1. Human and mouse samples

Human osteochondroma samples ($n = 12$) were obtained from biobanks of clinical pathology samples. All patients are Asians. These samples include 11 cases of solitary osteochondroma and one case of HME. All osteochondromas grew on the bone surface according to the medical record. Other characteristics of patients are summarized in Table 1. All experiments using human samples were performed in accordance with the Declaration of Helsinki and approved by an Institutional Review Board of Peking University Health Science Center (approval #: PKUSSIRB-201839127).

The human periosteum was sampled from the ankle or clavicle during hardware removal surgery in adult bone fracture patients. The sample from each patient was split into two parts. One part was fixed and processed for histological evaluation and immunohistochemistry. Another part was used to cultivate periosteal progenitors.

Table 1
Characteristics of osteochondroma patients

Patient #	Age	Sex	Tumor location	Pathological diagnosis
1	12	F	Distal tibia, right	Osteochondroma
2	11	F	Distal femur, right	Osteochondroma, multiple
3	10	M	Fibula, left	Osteochondroma
4	13	F	Femur, left	Osteochondroma
5	11	M	Proximal humerus, left	Osteochondroma
6	20	M	Ilium, right	Osteochondroma
7	35	F	Condyle, left mandibule	Osteochondroma
8	65	F	Condyle, right mandibule	Osteochondroma
9	29	F	Condyle, left mandibule	Osteochondroma
10	50	F	Condyle, left mandibule	Osteochondroma
11	24	F	Condyle, right mandibule	Osteochondroma
12	28	F	Condyle, left mandibule	Osteochondroma

Mouse samples were acquired from *Nfatc1-Cre;Rosa26*-mTmG$^{fl/+}$ and *Nfatc1-CreER^{T2};Rosa26-RFP$^{fl/+}$* reporter mice as described in the previous study [13]. *Nfatc1-CreER^{T2};Rosa26-RFP$^{fl/+}$* mice were pulsed with tamoxifen at 1 mg/10 g body weight for 5 consecutive days at 8 weeks of age and skeletal samples were harvested 48 h (hrs) later. The preparation of mouse bone samples for the analysis of fluorescence-labeled periosteal cells was described previously [13]. All animal studies were approved by the Institutional Animal Care and Use Committee of Capital Medical University (protocol #: AEEI-2022-036).

2.2. Immunohistochemistry

Serial sections were selected at 80–100 μm intervals and 6–12 sections were stained for each sample. Tissue was treated with EDTA antigen retrieval solution pH 8.0 at 70 °C overnight and incubated with primary antibodies: mouse anti-human NFATc1 (clone 7A6, Santa Cruz), rabbit anti-human/mouse NFATc2 (clone D43B1, Cell Signaling Technology), mouse IgG1κ isotype control (Cell Signaling Technology), or Rabbit IgG isotype control (Cell Signaling Technology) at 4 °C overnight, followed by secondary antibodies according to a Polink-2 plus®Polymer HRP Detection System (ZSGB-Bio, Beijing, China). All sections were counterstained with hematoxylin.

For evaluation and semi-quantification of immunohistochemistry results, NFATc1 positive and total counterstained cells were counted, respectively, for each region of interest (ROI). Three ROIs were randomly selected for each section. The scoring system is based on the average percentage of NFATc1 positive in total cells [24]: 0, no positive cells; 1, less than 10% positive cells; 2, more than 10% but less than 50% positive cells; 3, more than 50% positive cells. All samples were scored by two independent researchers.

2.3. Quantification of NFATc1-labeled cells in the human and mouse periosteum

To quantify NFATc1-labeled cells in the human and mouse periosteum, five serial slides with a 40 μm interval from each sample were used under the 40× objective and the cell counting module of a fluorescence microscope (BZ-×710, KEYENCE). For each slide, three random ROIs within the periosteum (only the cambium layer for the human periosteum) were selected for cell counting. Total cell numbers were counted with counterstained or DAPI-stained nuclei, and NFATc1-labeled cells were recognized by immunostained or RFP^{+} cells. The percentage of NFATc1-labeled cells in total cells was calculated.

2.4. Human periosteal progenitors

Human periosteal progenitors were isolated from fresh periosteal samples by combining enzyme digestion and explant culture. Briefly, periosteal tissues were rinsed in α-MEM supplemented with 2 mM L-glutamine, 100 U/ml penicillin-streptomycin, and 10% FBS three times, cut into small pieces, and digested with 3 mg/ml collagenase type I and 4 mg/ml dispase at 37 °C for 60 min. The digestion solution was cultured together with small tissue fragments for seven days and subcultured for two passages to eliminate slow-proliferating differentiated cells. The cells were then harvested, passed through a 70 μm strainer, and stained with APC anti-human CD31 (clone WM59, Biolegend) and APC anti-human CD45 (clone HI30, Biolegend) antibodies. CD45^{-}CD31^{-} non-hematopoietic, non-endothelial cells were sorted for further analyses (FACSAria™ II cell sorter, BD Bioscience).

2.5. Colony formation unit assay

The single cell suspension of sorted CD45^{-}CD31^{-} periosteal cells was seeded in 6-well plates at a density of 100 or 500 cells/well and cultured for two weeks. Cell colonies were stained with 1% crystal violet for 5 min after fixation in 10% neutral formalin for 15 min. Colonies (>50 cells) were counted under the microscope as previously described [13].

2.6. Ex vivo osteogenesis and adipogenesis

For osteogenesis and adipogenesis, human periosteal cells were seeded in 6-well plates at a density of 500 cells/well and cultured for two weeks to form cell colonies. Osteogenic medium (αMEM supplemented with 10% FBS, 10 nM dexamethasone, 50 μg/ml L-ascorbic acid and 10 mM β-glycerophosphate) or adipogenic medium (αMEM supplemented with 10% FBS, 100 nM dexamethasone, 50 μM indomethacin, and 5 μg/ml insulin) was then added to induce osteogenesis or adipogenesis for 3–4 weeks. Alizarin red and oil red O staining were used to visualize calcium nodules and fat, respectively.

2.7. Ex vivo chondrogenesis

Ex vivo chondrogenesis was analyzed using a 3D cell pellet culture system. Briefly, cells (1×10^6) were centrifuged to form pellets in 15 ml polypropylene tubes and cultured overnight. Chondrogenic medium (DMEM high glucose supplemented with 2% FBS, 100 nM dexamethasone, 50 μg/ml L-ascorbic acid, 1% insulin, transferrin, selenium (ITS), 1 mM sodium pyruvate, 40 μg/ml L-proline, and 10 ng/ml TGF-β1) was added the next day to induce chondrogenesis for 3 weeks. Cell pellets were fixed in 10% formalin and subjected to histological analysis. Alcian blue staining was used to evaluate chondrogenesis.

2.8. In vivo transplantation of human periosteal progenitors

Human periosteal progenitors (5.0×10^6) together with beta-tricalcium phosphate (SynthoGraft) were transplanted into the

dorsum of mice with severe combined immunodeficiency (SCID) through a tiny skin incision (<1 cm). Cell-free beta-tricalcium phosphate was used as the control. The transplants were harvested 5 weeks later and subjected to histological analysis after fixation in 10% formalin.

2.9. Flow cytometry

The following antibodies were used for flow cytometry: APC anti-human CD90 (clone 5E10, Biolegend), APC Mouse IgG1, κ isotype control (clone MOPC-21, Biolegend); PE anti-human CD51 (clone NKI-M9, Biolegend), PE Mouse IgG2a, κ isotype control (clone MOPC-173, Biolegend). Briefly, cells were incubated with specific antibodies or IgG isotype controls at room temperature for 30 min and then analyzed on a flow cytometer (FACSCalibur™ or BD LSR II, BD Bioscience). Both unstained and IgG isotype stained cells were referenced to gate positive cells. Data were analyzed using FlowJo software (Tree Star Inc.).

2.10. Western blotting

Fifty micrograms of protein from each sample were loaded for Western blotting analysis using 4–20% Mini-PROTEAN® TGX™ precast protein gels and *anti*-NFATc1 (1:1000, clone 7A6, Santa Cruz) or *anti*-GAPDH (1:2000, Cell Signaling Technology) antibody.

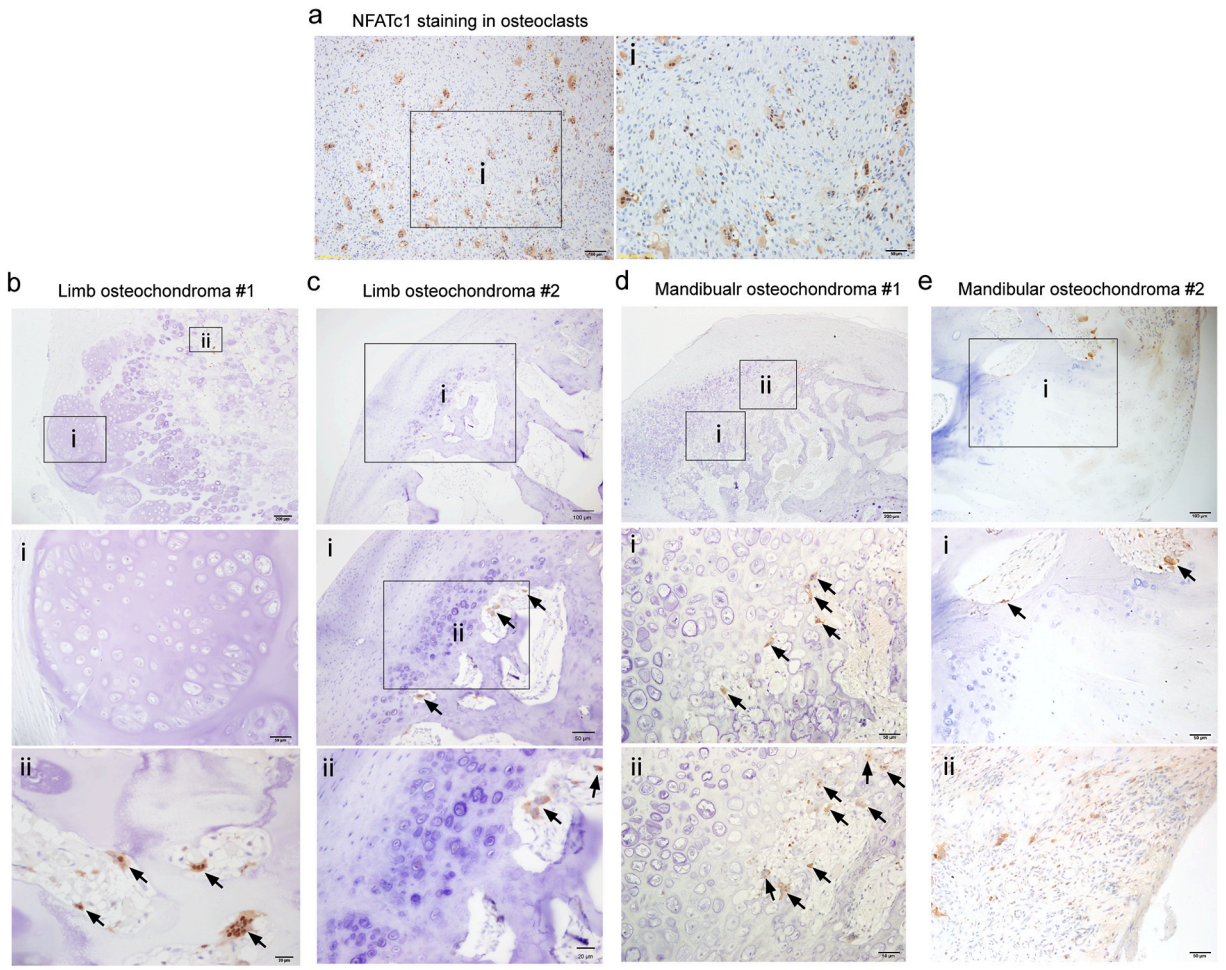

Fig. 1. Expression of NFATC1 in human osteochondromas. **a.** Immunohistochemistry of NFATC1 in a human Cherubism sample showing the specific staining of the NFATc1 antibody in osteoclasts. The image on the right (i) is the magnification of the rectangular region in the image on the left. $n = 3$ patients. **b-c.** Representative images of immunohistochemistry of NFATC1 in limb osteochondromas of two patients ($n = 4$ patients). Images i and ii are the magnification of rectangular regions in the upper images in each panel. Arrows indicating NFATC1-stained osteoclast-like cells in the underlying marrow space. ***d*-e.** Representative images of immunohistochemistry of NFATC1 in mandibular osteochondromas of two patients ($n = 5$ patients). Images i and ii are the magnification of rectangular regions in the upper images. Image ii in panel (**e**) showing NFATC1 staining in periosteum-like fibrous tissues adjacent to the osteochondroma. Arrows indicating NFATC1-stained osteoclast-like cells in the underlying marrow space. Scale bars as indicated in each image.

2.11. Statistics

Data were presented as mean ± standard deviation (s.d.). Statistical analyses were performed using Prism 9.2.0 (GraphPad). An unpaired, two-tailed student's *t*-test or nonparametric Mann-Whitney test was performed.

3. Results

3.1. Lack of NFATC1 expression in human osteochondroma cells

To examine the expression of NFATC1 in human osteochondroma cells, we retrieved 6 osteochondroma samples from limb skeletons and 6 osteochondroma samples from mandible bone from biobanks of clinical pathology samples (Table 1). Except for one of

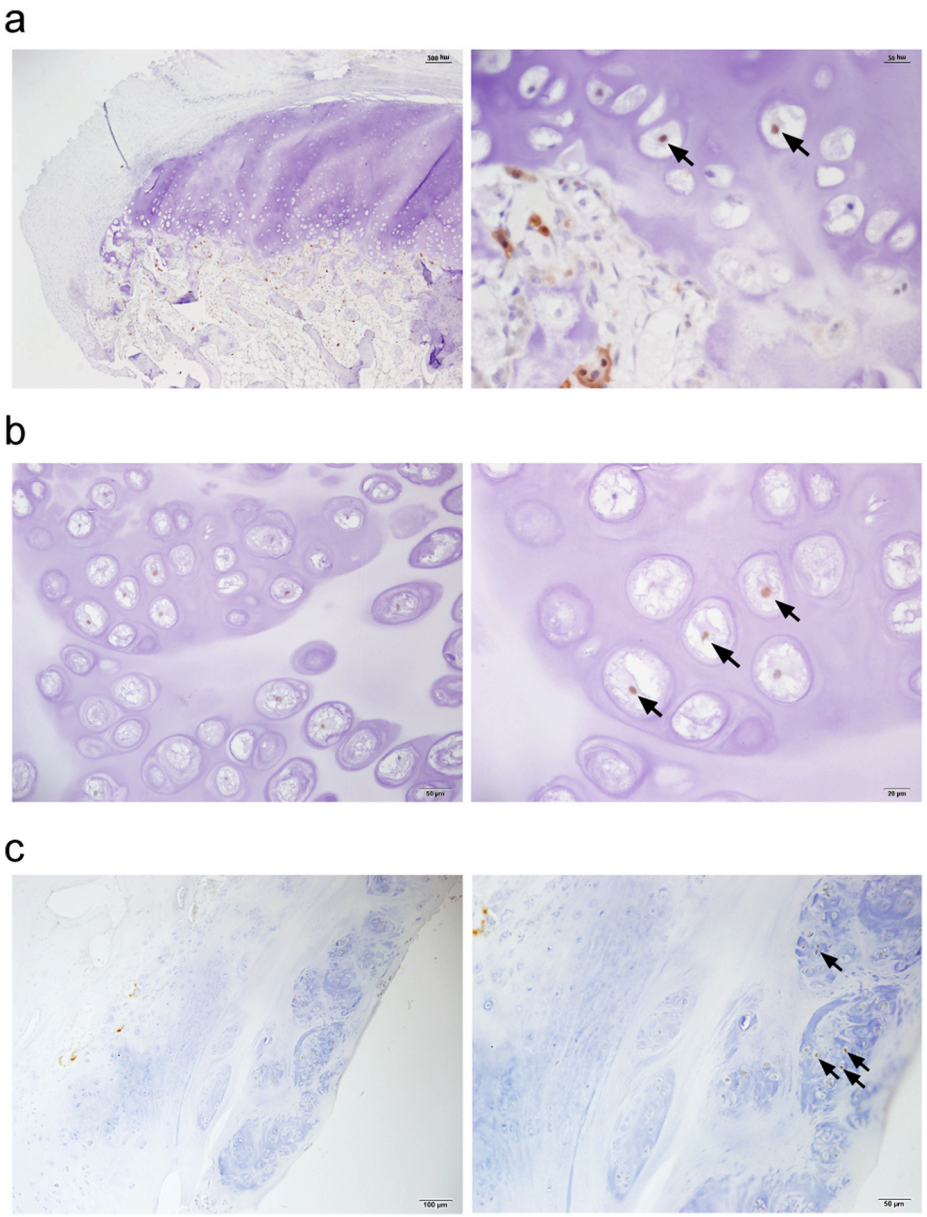

Fig. 2. Cellular heterogeneity of NFATC1 expression in human osteochondromas. **a.** Representative images showing the expression of NFATC1 in the nuclei of hypertrophic chondrocytes (arrows) in a limb osteochondroma. **b-c.** Representative images showing NFATC1 expression in the nuclei of clonally-grown chondrocytes (arrows) in osteochondromas from two patients (**b**, limb osteochondroma; **c**, mandibular osteochondroma). The right image is the magnification of part of the left image in each panel. Scale bars as indicated in each image.

these samples from the distal femur of a female patient with HME, all other samples were solitary osteochondromas. While the cases of osteochondromas of the limb skeleton included 3 male and 3 female patients, all osteochondroma samples of the mandibular bone came from women. In particular, the ages of patients undergoing surgery to remove these bone tumors were significantly younger in limb osteochondromas (10–20 years) compared to osteochondromas of the mandibular bone (24–65 years).

Before detecting NFATC1 expression in human osteochondroma specimens by immunohistochemistry, we first identified a positive control for NFATC1 expression by retrieving human Cherubism samples, as Cherubism is an osteoclast-enriched disease and NFATC1 is well characterized for its roles in osteoclast differentiation and functions [6,25]. The results showed that NFATC1 was specifically stained in multinucleated osteoclasts with a strong stain in the nuclei and a weak stain in the cytoplasm (Fig. 1a). NFATC1 was also stained in some single nucleated cells in human Cherubism samples, which could represent immune cells, since Cherubism is an inflammatory bone disorder [6]. These results demonstrate that osteoclasts represent a feasible positive control to assess NFATC1 expression in human osteochondromas.

For the immunohistochemistry of NFATC1 in human osteochondroma samples, we were unable to obtain reliable staining for 3 of the 12 osteochondroma cases because all sections fell off slides during the experimental procedure. The results of the remaining nine cases of human osteochondroma showed a general negative expression of NFATC1 in the superficial fibrous layer and most chondrocytes in the cartilaginous cap, while positive staining of NFATC1 was detected in multinucleated osteoclasts in the underlying marrow space (Fig. 1 b-e). As an alternative positive control, periosteum-like tissues were found near the tumor in one of the six osteochondroma cases of the mandibular bone, and positive staining of NFATC1 was found in multinucleated osteoclast-like cells and some single nucleated cells within fibrous tissues (Fig. 1e). The negative staining of NFATC1 in osteochondroma cells was not due to technical pitfalls of our immunohistochemistry methodology, such as an inappropriate antigen retrieval method for osteochondroma tissue, because a small proportion of NFATC1 positive chondrocytes were found in 7 of the 9 osteochondroma samples using the same experimental procedure (Fig. 2a).

In particular, relatively more NFATC1 positive chondrocytes could be found in clonally grown chondrocytes within the cartilaginous cap of osteochondromas (Fig. 2 b,c), reflecting the cellular heterogeneity regarding NFATC1 expression in human osteochondromas. Lastly, the results of the immunohistochemistry of NFATC1 were further evaluated using a semiquantified method based on the percentage of cells positive for NFATC1 and summarized in Table 2. Overall, these results demonstrate a lack of NFATC1 expression in the cartilaginous cap of human osteochondromas. The small proportion of NFATC1 positive chondrocytes suggests a mosaic distribution of NFATC1 negative and -positive chondrocytes in human osteochondromas, which is similar to the distribution of NFATc1-expressing cells in mouse osteochondromas and EXT1-expressing cells in human osteochondromas [13,26,27].

3.2. NFATC2 expression pattern in human osteochondromas

NFATc2 plays a complementary role to NFATc1 in determining the severity and number of mouse osteochondromas [13]. Therefore, we also examined the expression of NFATC2 in human osteochondroma samples by immunohistochemistry. The expression of NFATC2 was absent in most osteochondroma chondrocytes, while it could be detected in cells of the superficial fibrous layer or within the underlying marrow space (Fig. 3 a-c). In particular, NFATC2 expression in cells of the superficial fibrous layer of osteochondromas was contrasted to the absence of NFATC1 expression in these cells (Fig. 3a), but this disparity is consistent with the complementary roles of these two transcriptional factors in the formation of mouse osteochondroma: NFATC1 preferentially regulates skeletal progenitor cell proliferation and chondrogenesis, which occurs in the early stage of osteochondromagenesis, while NFATC2 is mainly responsible for chondrocyte hypertrophy and ossification at the late stage of osteochondromagenesis [13]. Therefore, the expression patterns of NFATC1 and NFATC2 in human osteochondroma samples agree with the complementary roles of these two transcriptional factors in osteochondromagenesis.

3.3. Localization of NFATC1 in the mouse and human periosteum

Our previous study in mouse models showed that NFATc1 identifies entheseal progenitors in the periosteum. Notably, in *Nfatc1-Cre;Rosa26*-mTmG$^{fl/+}$ mice, most periosteal cells are GFP^{+} at 8 weeks of age (Fig. 4a), suggesting that periosteal cells also express NFATc1 or are derived from progenitors that expressed NFATc1. Using tamoxifen-induced *Nfatc1-CreER^{T2};Rosa26-RFP$^{fl/+}$* reporter

Table 2
Summary of NFATC1 immunohistochemistry in human osteochondromas

Regions of interest	Frequency	Score
Superficial fibrous layer	0/9	0
Chondrocytes, non-clonal	4/6	1
Chondrocytes, clonal	3/3	2
Osteoclasts in the underlying marrow space	9/9	3
Nearby fibrous tissue	1/1	2

1. The word “non-clonal” or “clonal” represents whether chondrocytes grow in the clonal fashion.
2. Frequency X/Y means that there are X number of samples among the total Y number of samples that show positive NFATc1 staining.
3. Scoring standards: 0, no positive staining; 1, less than 10% of cells showing positive staining; 2, more than 10% but less than 50% of cells showing positive staining; 3, more than 50% of cells showing positive staining.

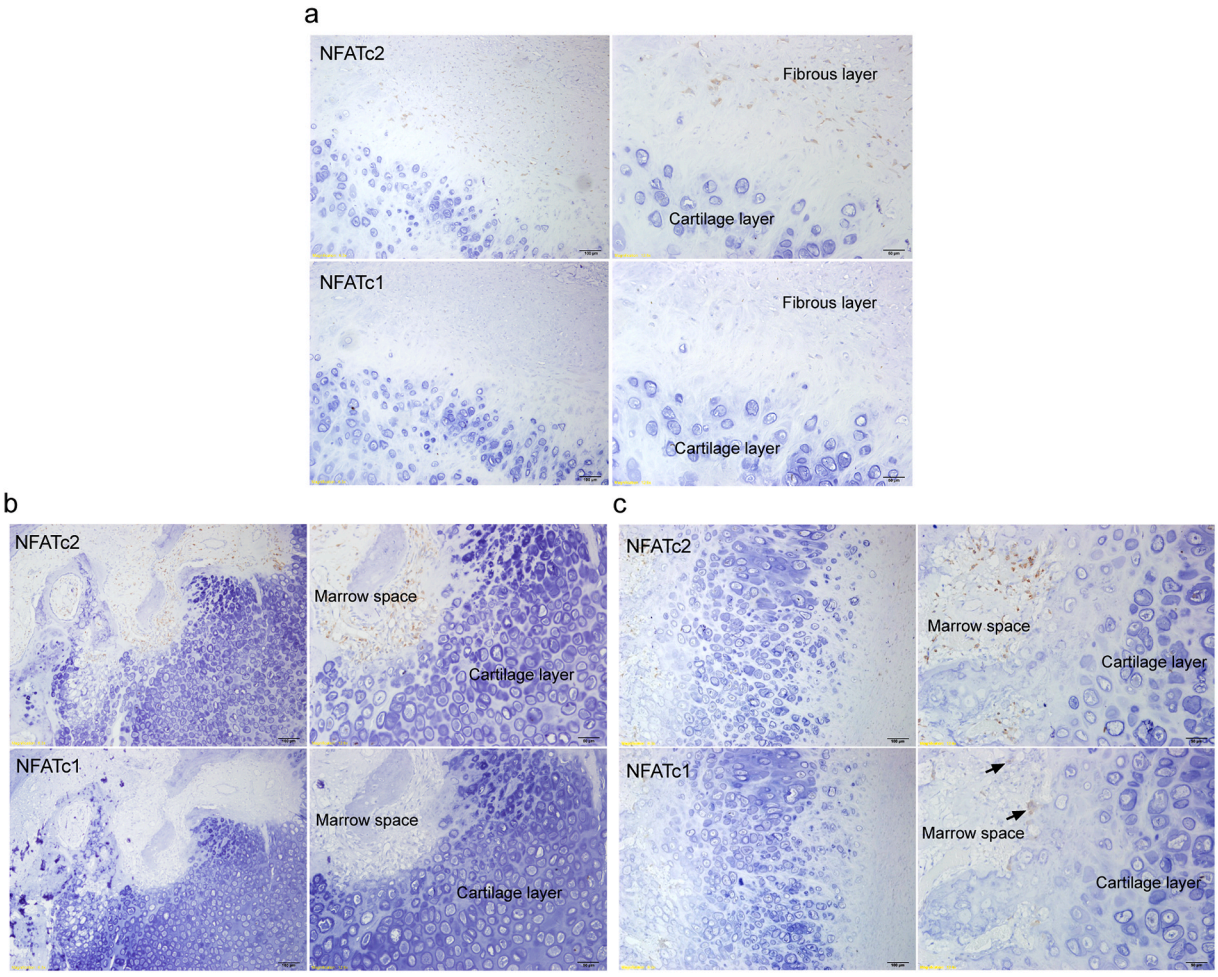

Fig. 3. Expression of NFATC2 in human osteochondromas. **a.** Representative images of NFATC2 immunohistochemistry showing positive staining in the superficial fibrous layer and negative staining in chondrocytes of human osteochondromas. The staining of NFATC1 was also shown for the same sample. **b-c.** Representative images of immunohistochemistry showing the absence of NFATC2 expression in chondrocytes of human osteochondromas, but positive staining in cells in the underlying marrow space. The staining of NFATC1 was also demonstrated for the same sample. Arrows indicated osteoclast-like cells stained for NFATC1. The right image is the magnification of part of the left image in each panel. Scale bars: left panel, 100 μm; right panel, 50 μm.

mice, we found that NFATc1 expression was only localized in a portion of periosteal cells at 8 weeks of age shortly after the tamoxifen pulse (Fig. 4a). Combining lineage tracing data in *Nfatc1-Cre;Rosa26*-mTmG$^{fl/+}$ and *Nfatc1-CreER^{T2};Rosa26-RFP$^{fl/+}$* mice, cells expressing NFATc1 (RFP^{+}) in the periosteum of *Nfatc1-CreER^{T2};Rosa26-RFP$^{fl/+}$* mice should be periosteal progenitors and cells not expressing NFATc1 should be differentiated periosteal cells such as fibroblasts and osteoblasts. Therefore, many GFP $^{+}$ cells in the periosteum of *Nfatc1-Cre;Rosa26*-mTmG$^{fl/+}$ mice could arise from periosteal progenitors that expressed NFATc1 and had been depredated of the expression of NFATc1 with development.

To explore the expression of NFATC1 in the human periosteum, we obtained human periosteal tissues from the region near the bone fracture healing site during hardware removal surgery. Histology (H&E staining) was performed first to evaluate the morphology of the human periosteum. Consistent with previous reports [28–30], the human periosteum was composed of two tissue layers: fibrous and cambium (Fig. 4b). While the fibrous layer was thicker, the cambium layer was highly cellular. The cambium layer of the human periosteum has been considered the primary location where periosteal progenitors reside and also contains other cell types such as pre-osteoblasts, differentiated osteoblasts, fibroblasts, and pericytes [28,30]. It should be noted that the periosteum near the bone fracture healing site is likely thicker than the normal human periosteum at the time of hardware removal surgery and also contains certain inflammatory cells due to tissue growth and remodeling. The immunohistochemistry of NFATC1 showed that a portion of cells in the cambium layer was positively stained with the NFATc1 antibody. In particular, the ratio of NFATC1 positive cells in human periosteal tissue was comparable to that of RFP $^{+}$ cells in the periosteum of adult *Nfatc1-CreER^{T2};Rosa26-RFP$^{fl/+}$* mice after pulse of tamoxifen (11.04 ± 2.05% *vs.* 9.56 ± 0.80%, $P = 0.3101$, Fig. 4c). These results demonstrate the localization of NFATC1 in both the mouse and the human periosteum.

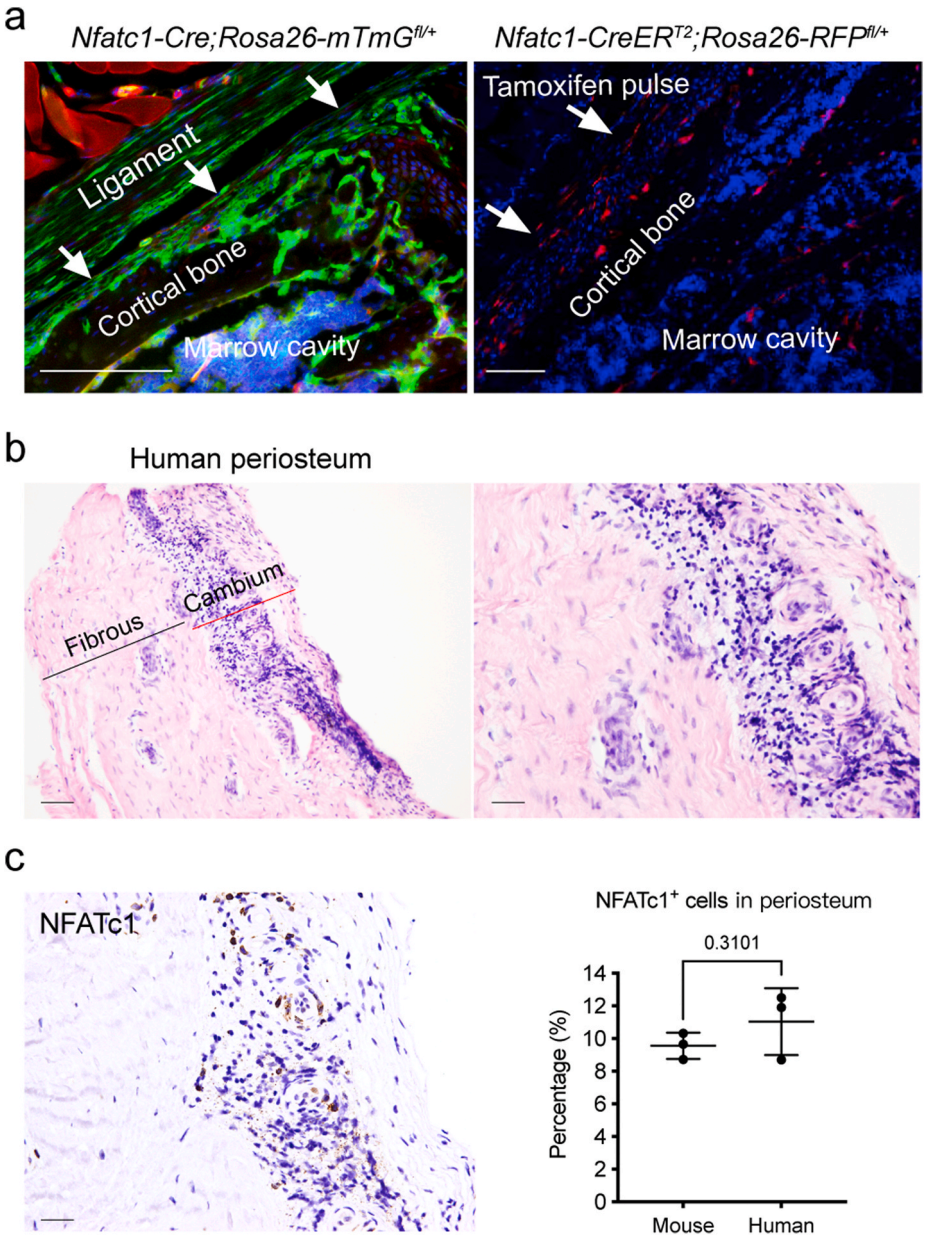

Fig. 4. NFATC1 is localized in both the mouse and the human periosteum. **a.** Fate-mapping of NFATc1-expressing cells in the periosteum of *Nfatc1-Cre;Rosa26*-mTmG$^{fl/+}$ mice (GFP^{+} cells in the left panel) and localization of real-time expression of NFATc1 in the adult periosteum in *Nfatc1-CreER^{T2};Rosa26-RFP$^{fl/+}$* mice 48 hrs after tamoxifen pulse for 5 consecutive days (RFP^{+} cells in the right panel). Arrows indicate periosteum on the surface of cortical bone. $n = 5$ *Nfatc1-Cre;Rosa26*-mTmG$^{fl/+}$ mice and 3 *Nfatc1-CreER^{T2};Rosa26-RFP$^{fl/+}$* mice. Scale bars: 200 μm. **b.** Representative hematoxylin and eosin (H&E) images of adult human periosteal tissues obtained from the ankle during hardware removal surgery of bone fracture healing patients showing the two-layer structure of the periosteum: fibrous and cambium. The right image is a magnification of part of the left image. Scale bars: left, 50 μm; right, 25 μm. **c.** Immunohistochemistry of NFATC1 in the human periosteum and quantifying the percentage of cells labeled with NFATC1 in the cambium layer. The percentage of cells labeled with NFATc1 in the mouse periosteum (RFP^{+} cells in the right panel in (**a**) was used as a control. Data are mean ± SD, two-tailed student's *t*-test. $n = 3$ human or mouse donors, five serial sections per sample, and three random regions of interest (ROIs) in each section. Scale bar, 25 μm.

3.4. NFATC1 is enriched in human periosteal progenitors

To explore the expression of NFATC1 in human periosteal progenitors, we isolated progenitor cells from the human periosteum to examine the expression of NFATC1 compared to human bone marrow stromal cells (BMSC). Human periosteal progenitors were isolated by combining enzyme digestion and explant culture, which could significantly enhance the abundance of progenitor cells

according to our pilot studies (Fig. 5a). After subculture for two passages to eliminate slow-dividing differentiated cells [31], $CD45^{-}CD31^{-}$ non-hematopoietic, non-endothelial, and plastic-adherent cells were sorted for further analysis (Fig. 5b). First, the colony-forming unit assay showed that the sorted periosteal mesenchymal cells contained abundant cells with clonogenic capacity and the grown cell colonies were heterogeneous in size and cell density, reflecting the heterogeneity in cell proliferation (Fig. 5c). Second, under appropriate lineage-specific differentiation conditions, these periosteal cells could be induced toward osteogenesis and adipogenesis *in vitro,* but showed a weak potential for chondrogenesis, as shown by alizarin red, oil red O, or alcian blue staining, respectively (Fig. 5d). Consistently, when transplanted together with β-tricalcium phosphate underneath the dorsal skin of SCID mice, these periosteal cells formed ossicles through intramembranous ossification, and chondrocytes were not found in these tissues, as

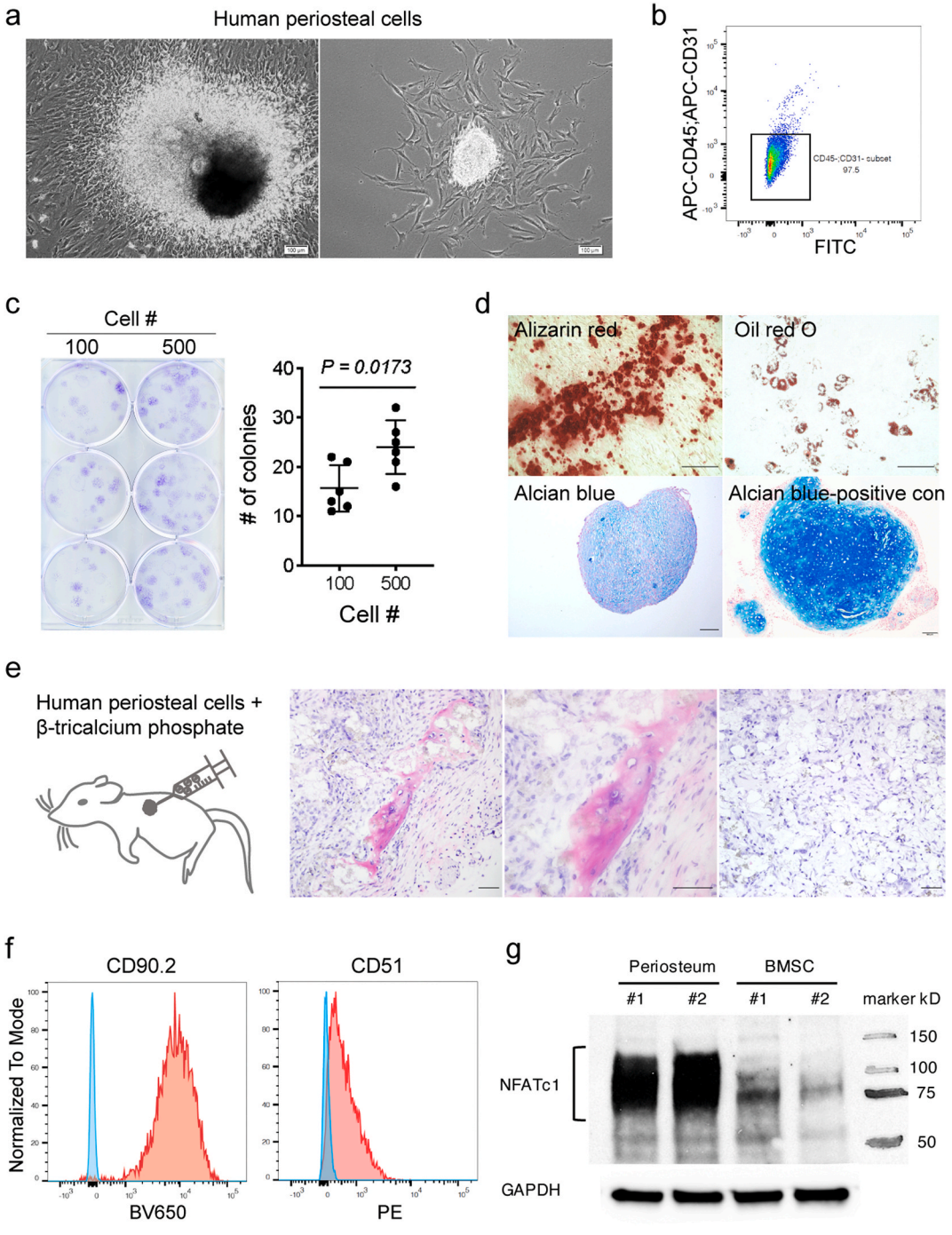

(caption on next page)

Fig. 5. NFATC1 is enriched in human periosteal progenitors. **a.** Representative phase-contrast images of human periosteal progenitor cell culture. **b.** Representative dot-plot image of fluorescence-activated cell sorting (FACS) of $CD45^{-}CD31^{-}$ non-hematopoietic, non-endothelial periosteal cells (97.5%). **c.** Colony formation unit assay of human periosteal cells. Cells were plated at indicated numbers and cultured for 2 weeks. Colonies were stained with 1% crystal violet. Data are mean ± SD, Mann-Whitney test. $n = 2$ human donors, 3 replicates for each at each cell density. **d.** Trilineage differentiation potentials of human periosteal progenitors. The capacity of osteogenesis, adipogenesis, and chondrogenesis was displayed by alizarin red, oil red O, and alcian blue staining, respectively. NFATc1-expressing progenitors sorted from the knee of neonatal *Nfatc1-Cre;Rosa26*-$mTmG^{fl/+}$ mice were used as a positive control for chondrogenesis. Scale bars, 100 μm. **e.** *In vivo* transplantation of human periosteal progenitors. Left panel, schematic showing transplantation of human periosteal cells with β-tricalcium phosphate to the dorsum of mice with severe combined immunodeficiency (SCID). Middle 2 panels, representative H&E staining showing ossicle formation 5 weeks after *in vivo* transplantation (the right image is the magnification of part of the left image). Most right panel, H&E staining of tissues 5 weeks after only transplanting β-tricalcium phosphate. $n = 2$ human donors, 5 animals for each. Scale bars, 50 μm. **f.** Representative flow cytometry results of the examination of cell surface markers CD90 and CD51 in human periosteal progenitor cells. **g.** Western blotting determining the expression of NFATC1 in human periosteal progenitors relative to bone marrow stromal cells (BMSC), uncropped images referencing Supplementary Fig. 1.

evaluated by two independent experienced pathologists (Fig. 5e). The ossicle was not observed when only β-tricalcium phosphate was transplanted.

CD90 has been shown as a surface molecular marker of periosteal progenitors, and periosteum-derived cells sorted by CD90 showed higher proliferative capacity and osteogenic potential compared to unsorted cells [32,33]. Throughout, the vast majority of cells derived from the periosteum we cultured were positive for CD90 (Fig. 5f). Furthermore, a major proportion of these periosteal cells also expressed another periosteal progenitor cell surface marker, CD51 (Fig. 5f) [33]. Therefore, the periosteal cells we isolated represent a progenitor-enriched population. Next, the results of Western blotting showed that these human periosteal progenitors expressed a much higher level of NFATC1 compared to human BMSC matched in age and sex (Fig. 5g and Supplementary Fig. 1), suggesting that NFATC1 is enriched in human periosteal progenitors. Taken together, these results demonstrate an enriched expression of NFATC1 in human periosteal progenitors and highlight the role of NFATC1 in identifying skeletal progenitors.

4. Discussion

In this study, in contrast to the enriched expression of NFATC1 in human periosteal progenitors, the lack of NFATC1 expression was observed in most cells in the cartilaginous cap of human osteochondromas, suggesting that NFATC1 expression might be suppressed during human osteochondromagenesis. The NFATC2 protein is also undetectable in most human osteochondroma chondrocytes. These results are consistent with our previous findings in mouse models that NFATc1 and NFATc2 restrict osteochondromagenesis from entheseal progenitors [13] and provide critical translational insights in the human setting. Notably, the enthesis is essentially a portion of the periosteum, and the periosteum/perichondrium has been considered the main origin of cells for osteochondroma formation [18]. Therefore, it is rational to consider periosteal progenitors as the control for osteochondroma cells.

In recent decades, studies on the pathogenesis of osteochondromas have made great progress [19]. Except for the mutations of the EXT1 and/or EXT2 genes, there should be other events that cause or contribute to the formation of osteochondromas, as heterogeneous mutations of EXT1 or EXT2 are not enough to initiate osteochondromagenesis. The loss of heterozygosity in EXT mutations has been proposed as one of these events that initiates the osteochondromagenesis process [27,34]. Furthermore, our recent findings in mice knocked out of NFATc1 and NFATc2 reveal that impaired NFAT signaling could also represent a causative event for osteochondroma formation [13]. In the present study, the expression patterns of NFATC1 and NFATC2 in human osteochondroma samples are consistent with the inhibitory role of NFAT signaling in osteochondromagenesis. However, the relationship between NFAT and EXT genes in osteochondromagenesis remains unclear. Our previous study did not find changes in *Ext1* and *Ext2* gene expression in mouse skeletal progenitors deficient in NFATc1 and/or NFATc2 [13], indicating that NFATc1 and NFATc2 do not function as direct transcriptional activators of the EXT genes. Rather, it is possible that EXT gene mutations affect heparan sulfate formation and then activate molecular signaling that inhibits the expression or activity of NFATs to cause osteochondroma formation. Inactivation of NFATc1 and/or NFATc2 could also occur independently of EXT signaling during osteochondromagenesis, responsible for osteochondroma cases without mutations in the EXT1 or EXT2 gene. Future studies will further characterize the potential crosstalk between the NFAT and EXT genes during osteochondroma formation.

Another limitation of the present study is that we did not examine the functions of the EXT1 and EXT2 genes in these human osteochondroma samples due to the lack of a specific antibody for heparan sulfate, nor do we have information on the mutations of the EXT genes in these human osteochondroma samples. Future studies need to identify an available antibody for heparan sulfate to examine the function of the EXT genes and define the crosstalk between the NFAT and EXT genes during osteochondroma formation.

Previous results in mouse models show that NFATc1 is necessary to inhibit overproliferation or maintain quiescence of skeletal progenitors by suppressing *c-Myc* expression and promoting the expression of the cyclin-dependent kinase inhibitor *p21* [13]. Furthermore, NFATc1 negatively regulates chondrogenesis of skeletal progenitors by affecting *Col2a1* and *Col10a1* expression, while NFATc2 primarily controls the ossification process and osteogenesis by regulating *Mmp13* and *Ibsp* expression [13]. As our results in the current manuscript demonstrate that NFATC1 and NFATC2 could have a similar function in regulating human osteochondromagenesis, it will be necessary to further explore the mechanism of NFATC1 and NFATC2 in regulating osteochondroma formation, including their upstream and downstream signaling, and whether the expression or activity of NFATC1 and NFATC2 are simultaneously or sequentially inactivated. It should be noted that a previous study showed that neither $Nfatc3^{Col2}$ nor $Nfatc3^{Col2}Nfatc2^{-/-}$ mice exhibit any cartilage phenotypic abnormalities at the histological and clinical levels [5], suggesting that NFATc3, unlike NFATc1,

may be dispensable and does not have a complementary role with NFATc2 in cartilage biology and osteochondromagenesis.

The heterogeneity of osteochondroma cells has been widely appreciated in previous studies [18,26,35]. Most osteochondroma patients carry mutations on one allele of the EXT1 or/and EXT2 genes and the occurrence of osteochondromas needs a second hit, such as 'loss of heterozygosity' or other genetic events, to further lower the level of heparan sulfate (not necessary for total loss of its expression). In mouse models deficient in NFATs, the cartilaginous cap of osteochondromas contains mixed cells of NFATc1-deficient and -sufficient cells [13]. Similarly, a small proportion of NFATC1-positive hypertrophic chondrocytes was detected in 7 of 9 osteochondroma cases (Fig. 2 and Table 2), indicating that human osteochondromas may contain a similar mosaic distribution of NFATC1 negative and positive cells. Notably, although we did not quantitatively compare the ratio of NFATC1-positive to that of EXT1 positive cells in human osteochondromas, the number of NFATC1 positive cells is significantly lower than that of EXT1 positive cells from previous reports [21].

The periosteum is critical for bone development, homeostasis, and repair [36]. Many skeletal diseases, including benign and malignant bone tumors, can be the periosteum of origin [37]. The periosteal progenitors and BMSC have different molecular markers and demonstrate different regenerative capacities during bone fracture healing [38,39]. The periosteum/perichondrium has been considered one of the primary sources of cells for osteochondroma formation [18,40]. Our results in the present study show an enriched expression of NFATC1 in human periosteal progenitors, suggesting that NFATC1 plays a role in the biology of periosteum and related diseases. As mentioned above, the upstream and downstream mechanisms of NFATC1 in regulating periosteal progenitor cell differentiation and related diseases remain unclear and warrant further studies.

In summary, the expression patterns of the NFATC1 and NFATC2 proteins in human osteochondroma cells endorse an inhibitory role of NFAT signaling in osteochondromagenesis, providing a basis for further exploration of the mechanism of NFAT signaling regulating human osteochondromagenesis.

Author contribution statement

Yuanyuan Wang: Performed the experiments; Analyzed and interpreted the data.

Jiangdong Ren, Guojin Hou: Contributed reagents, materials, analysis tools or data.

Xianpeng Ge: Conceived and designed the experiments; Performed the experiments; Analyzed and interpreted the data; Wrote the paper.

Funding statement

Dr. Xianpeng Ge was supported by National Natural Science Foundation of China [81100767], Beijing Natural Science Foundation [5222008], Natural Science Foundation of Capital Medical University [1220010146], Outstanding Young Researcher Award of Beijing Municipality, and Outstanding Researcher Award of Xuanwu Hospital.

Data availability statement

Data included in article/supp. Material/referenced in article.

Declaration of interest's statement

The authors declare that they have no known competing financial interests or personal relationships that could have appeared to influence the work reported in this paper.

Acknowledgements

The authors thank Dr. Ruirui Shi for providing samples and collecting parts of these data, and Dr. Haiyan Luo for histological evaluation.

Appendix A. Supplementary data

Supplementary data related to this article can be found at https://doi.org/10.1016/j.heliyon.2023.e13018.

References

[1] A. Rao, C. Luo, P.G. Hogan, Transcription factors of the NFAT family: regulation and function, Annu. Rev. Immunol. 15 (1997) 707–747.
[2] S. Chuvpilo, E. Jankevics, D. Tyrsin, A. Akimzhanov, D. Moroz, M.K. Jha, J. Schulze-Luehrmann, B. Santner-Nanan, E. Feoktistova, T. Konig, et al., Autoregulation of NFATc1/A expression facilitates effector T cells to escape from rapid apoptosis, Immunity 16 (6) (2002) 881–895.
[3] P.G. Hogan, L. Chen, J. Nardone, A. Rao, Transcriptional regulation by calcium, calcineurin, and NFAT, Genes Dev. 17 (18) (2003) 2205–2232.
[4] M. Vaeth, S. Feske, NFAT control of immune function: New Frontiers for an Abiding Trooper, F1000Res 7 (2018) 260.

[5] M.B. Greenblatt, S.Y. Ritter, J. Wright, K. Tsang, D. Hu, L.H. Glimcher, A.O. Aliprantis, NFATc1 and NFATc2 repress spontaneous osteoarthritis, Proc. Natl. Acad. Sci. U. S. A. 110 (49) (2013) 19914–19919.
[6] A.O. Aliprantis, Y. Ueki, R. Sulyanto, A. Park, K.S. Sigrist, S.M. Sharma, M.C. Ostrowski, B.R. Olsen, L.H. Glimcher, NFATc1 in mice represses osteoprotegerin during osteoclastogenesis and dissociates systemic osteopenia from inflammation in cherubism, J. Clin. Invest. 118 (11) (2008) 3775–3789.
[7] D. Sitara, A.O. Aliprantis, Transcriptional regulation of bone and joint remodeling by NFAT, Immunol. Rev. 233 (1) (2010) 286–300.
[8] M.M. Winslow, M. Pan, M. Starbuck, E.M. Gallo, L. Deng, G. Karsenty, G.R. Crabtree, Calcineurin/NFAT signaling in osteoblasts regulates bone mass, Dev. Cell 10 (6) (2006) 771–782.
[9] A.M. Ranger, L.C. Gerstenfeld, J. Wang, T. Kon, H. Bae, E.M. Gravallese, M.J. Glimcher, L.H. Glimcher, The nuclear factor of activated T cells (NFAT) transcription factor NFATp (NFATc2) is a repressor of chondrogenesis, J. Exp. Med. 191 (1) (2000) 9–22.
[10] F. Nishigaki, S. Sakuma, T. Ogawa, S. Miyata, T. Ohkubo, T. Goto, FK506 induces chondrogenic differentiation of clonal mouse embryonic carcinoma cells, ATDC5, Eur. J. Pharmacol. 437 (3) (2002) 123–128.
[11] S. Zanotti, E. Canalis, Notch suppresses nuclear factor of activated T cells (NFAT) transactivation and Nfatc1 expression in chondrocytes, Endocrinology 154 (2) (2013) 762–772.
[12] C. Pilquil, Z. Alvandi, M. Opas, Calreticulin regulates a switch between osteoblast and chondrocyte lineages derived from murine embryonic stem cells, J. Biol. Chem. 295 (20) (2020) 6861–6875.
[13] X. Ge, K. Tsang, L. He, R.A. Garcia, J. Ermann, F. Mizoguchi, M. Zhang, B. Zhou, B. Zhou, A.O. Aliprantis, NFAT restricts osteochondroma formation from entheseal progenitors, JCI Insight 1 (4) (2016), e86254.
[14] L.W. Alabdullrahman, D.W. Byerly, in: Osteochondroma, StatPearls. edn. Treasure, Island (FL, 2020.
[15] M.D. Murphey, J.J. Choi, M.J. Kransdorf, D.J. Flemming, F.H. Gannon, Imaging of osteochondroma: variants and complications with radiologic-pathologic correlation, Radiographics 20 (5) (2000) 1407–1434.
[16] S. Mohanty, H. Gupta, J. Dabas, P. Kumar, Osteochondroma of maxillofacial region: tumor arising from two different developmental bones, J. Oral Maxillofac. Pathol. 20 (2) (2016) 329.
[17] S. Sinha, C. Mundy, T. Bechtold, F. Sgariglia, M.M. Ibrahim, P.C. Billings, K. Carroll, E. Koyama, K.B. Jones, M. Pacifici, Unsuspected osteochondroma-like outgrowths in the cranial base of Hereditary Multiple Exostoses patients and modeling and treatment with a BMP antagonist in mice, PLoS Genet. 13 (4) (2017), e1006742.
[18] M. Pacifici, Hereditary multiple exostoses: new insights into pathogenesis, clinical complications, and potential treatments, Curr. Osteoporos. Rep. 15 (3) (2017) 142–152.
[19] M. Pacifici, Hereditary multiple exostoses: are there new plausible treatment strategies? Expert Opin Orphan Drugs 6 (6) (2018) 385–391.
[20] A.H. Tessa, J.V.B. Wilpshaar, Bone: osteochondroma, Atlas Genet Cytogenet Oncol Haematol 23 (5) (2019) 133–136.
[21] C.E. de Andrea, C.M. Reijnders, H.M. Kroon, D. de Jong, P.C. Hogendoorn, K. Szuhai, J.V. Bovee, Secondary peripheral chondrosarcoma evolving from osteochondroma as a result of outgrowth of cells with functional EXT, Oncogene 31 (9) (2012) 1095–1104.
[22] M. Zuntini, E. Pedrini, A. Parra, F. Sgariglia, F.V. Gentile, M. Pandolfi, M. Alberghini, L. Sangiorgi, Genetic models of osteochondroma onset and neoplastic progression: evidence for mechanisms alternative to EXT genes inactivation, Oncogene 29 (26) (2010) 3827–3834.
[23] K.B. Jones, M. Pacifici, M.J. Hilton, Multiple hereditary exostoses (MHE): elucidating the pathogenesis of a rare skeletal disorder through interdisciplinary research, Connect. Tissue Res. 55 (2) (2014) 80–88.
[24] N. Fedchenko, J. Reifenrath, Different approaches for interpretation and reporting of immunohistochemistry analysis results in the bone tissue - a review, Diagn. Pathol. 9 (2014) 221.
[25] J. Southgate, U. Sarma, J.V. Townend, J. Barron, A.M. Flanagan, Study of the cell biology and biochemistry of cherubism, J. Clin. Pathol. 51 (11) (1998) 831–837.
[26] A. Cuellar, A.H. Reddi, Cell biology of osteochondromas: bone morphogenic protein signalling and heparan sulphates, Int. Orthop. 37 (8) (2013) 1591–1596.
[27] K.B. Jones, V. Piombo, C. Searby, G. Kurriger, B. Yang, F. Grabellus, P.J. Roughley, J.A. Morcuende, J.A. Buckwalter, M.R. Capecchi, et al., A mouse model of osteochondromagenesis from clonal inactivation of Ext1 in chondrocytes, Proc. Natl. Acad. Sci. U. S. A. 107 (5) (2010) 2054–2059.
[28] M.R. Allen, J.M. Hock, D.B. Burr, Periosteum: biology, regulation, and response to osteoporosis therapies, Bone 35 (5) (2004) 1003–1012.
[29] J.R. Dwek, The periosteum: what is it, where is it, and what mimics it in its absence? Skeletal Radiol. 39 (4) (2010) 319–323.
[30] G. Augustin, A. Antabak, S. Davila, The periosteum. Part 1: anatomy, histology and molecular biology, Injury 38 (10) (2007) 1115–1130.
[31] F. Hendijani, Explant culture: an advantageous method for isolation of mesenchymal stem cells from human tissues, Cell Prolif 50 (2) (2017).
[32] Y.K. Kim, H. Nakata, M. Yamamoto, M. Miyasaka, S. Kasugai, S. Kuroda, Osteogenic potential of mouse periosteum-derived cells sorted for CD90 in vitro and in vivo, Stem Cells Transl Med 5 (2) (2016) 227–234.
[33] X. Wang, B.G. Matthews, J. Yu, S. Novak, D. Grcevic, A. Sanjay, I. Kalajzic, PDGF modulates BMP2-induced Osteogenesis in Periosteal Progenitor Cells, JBMR Plus 3 (5) (2019), e10127.
[34] J.V. Bovee, EXTra hit for mouse osteochondroma, Proc Natl Acad Sci U S A 107 (5) (2010) 1813–1814.
[35] C.M. Reijnders, C.J. Waaijer, A. Hamilton, E.P. Buddingh, S.P. Dijkstra, J. Ham, E. Bakker, K. Szuhai, M. Karperien, P.C. Hogendoorn, et al., No haploinsufficiency but loss of heterozygosity for EXT in multiple osteochondromas, Am J Pathol 177 (4) (2010) 1946–1957.
[36] S.J. Roberts, N. van Gastel, G. Carmeliet, F.P. Luyten, Uncovering the periosteum for skeletal regeneration: the stem cell that lies beneath, Bone 70 (2015) 10–18.
[37] L. Lichtenstein, Tumors of periosteal origin, Cancer 8 (5) (1955) 1060–1069.
[38] O. Duchamp de Lageneste, A. Julien, R. Abou-Khalil, G. Frangi, C. Carvalho, N. Cagnard, C. Cordier, S.J. Conway, C. Colnot, Periosteum contains skeletal stem cells with high bone regenerative potential controlled by Periostin, Nat Commun 9 (1) (2018) 773.
[39] L.C. Ortinau, H. Wang, K. Lei, L. Deveza, Y. Jeong, Y. Hara, I. Grafe, S.B. Rosenfeld, D. Lee, B. Lee, et al., Identification of Functionally Distinct Mx1+alphaSMA + Periosteal Skeletal Stem Cells, Cell Stem Cell 25 (6) (2019) 784–796 e785.
[40] A. D'Arienzo, L. Andreani, F. Sacchetti, S. Colangeli, R. Capanna, Hereditary Multiple Exostoses: Current Insights, Orthop Res Rev 11 (2019) 199–211.